

# Multicritical absorbing phase transition in a class of exactly solvable models

Arijit Chatterjee\* and P. K. Mohanty

CMP Division, Saha Institute of Nuclear Physics, HBNI, 1/AF Bidhan Nagar, Kolkata 700064, India

(Received 29 September 2016; published 28 December 2016)

We study diffusion of hard-core particles on a one-dimensional periodic lattice subjected to a constraint that the separation between any two consecutive particles does not increase beyond a fixed value  $n + 1$ ; an initial separation larger than  $n + 1$  can however decrease. These models undergo an absorbing state phase transition when the conserved particle density of the system falls below a critical threshold  $\rho_c = 1/(n + 1)$ . We find that the  $\phi_k$ , the density of 0-clusters (0 representing vacancies) of size  $0 \leq k < n$ , vanish at the transition point along with activity density  $\rho_a$ . The steady state of these models can be written in matrix product form to obtain analytically the static exponents  $\beta_k = n - k$  and  $\nu = 1 = \eta$  corresponding to each  $\phi_k$ . We also show from numerical simulations that, starting from a natural condition,  $\phi_k(t)$ s decay as  $t^{-\alpha_k}$  with  $\alpha_k = (n - k)/2$  even though other dynamic exponents  $\nu_t = 2 = z$  are independent of  $k$ ; this ensures the validity of scaling laws  $\beta = \alpha \nu_t$  and  $\nu_t = z \nu$ .

DOI: [10.1103/PhysRevE.94.062141](https://doi.org/10.1103/PhysRevE.94.062141)

## I. INTRODUCTION

The absorbing state phase transition (APT) [1] is the most studied nonequilibrium phase transition in the past few decades. Unlike equilibrium counterparts, these systems do not obey the detailed balance condition, as the absorbing configurations of the system can be reached by the dynamics but cannot be left. Thus, by tuning a control parameter these systems can be driven from an active phase to an absorbing one where the dynamics cease. On the one hand, the nonequilibrium dynamics generically make analytical treatment of these systems highly nontrivial, giving rise to a varied class of distributions as well as a rich variety of novel correlations, and, on the other hand, the nonfluctuating disordered phase being unique to the APT leads to a unconventional critical behavior. The most robust universality class of the APT is directed percolation (DP) [2], which is observed in the context of synchronization [3], damage spreading [4], depinning transition [5], catalytic reactions [6], forest fire [7], extinction of species [8], etc. Recently, DP critical behavior was observed experimentally [9] in liquid crystals. It has been conjectured [10] that in the absence of any special symmetry or quenched randomness, the APT in systems following short-range dynamics, characterized by a non-negative fluctuating scalar order parameter, belongs to DP.

Models involving more than one species of particles can have interesting features [11,12]. Some of these models also show multicriticality in a sense that the density of different species may vanish at the critical point following power laws with different exponents. In the one-dimensional coupled directed percolation process [11], where the transmutation is unidirectional, the order-parameter exponents for different species are found to be  $\beta = 0.27, 0.11, \dots$ , with the first value being that of DP. A similar feature has been observed numerically in the roughening transition occurring in growth models with adsorption, and desorption at boundaries [13]. In the context of equilibrium, multicriticality has also been seen in models with multiple components, such as the binary

Ising model [14] and the Potts model [15]. In all these models the order-parameter field associated with each component vanishes simultaneously at some critical tuning parameter, resulting in multicriticality. In this article we aim at studying multicritical behavior in the context of the absorbing phase transition. We show that simple diffusion of hard-core particles on a lattice can undergo a multicritical absorbing phase transition when additional constraints or particle interactions are introduced; multiple order parameters turn out to be an emerging feature of this single-component system.

The model we investigate here is a variant of the assisted hopping models where hard-core particles hop to one of the neighbors with rates that generally depend on the distance of the moving particle from its nearest occupied neighbor [16–19]; steady-state weights of some of these models are known exactly [16,20,21]. We restrict the study only to a special case, where diffusion of particles is additionally constrained not to increase the interparticle separation beyond a fixed positive integer  $n + 1$ . The steady-state weights of the models in this class, parametrized by the integer  $n$ , can be written in matrix product form. This helps us obtain the spatial correlation functions exactly. In particular, the density of 0-clusters of size  $0 \leq k < n$  vanishes at the critical point following power laws with  $k$ -dependent exponents. Thus, the cluster density  $\phi_k$  for each  $k$  can be considered as order parameters of the system in addition to the natural order parameter  $\rho_a$ , namely, activity density. Our careful numerical study of the decay of  $\phi_k$  from a natural initial condition [22,23], which is hyperuniform [24], shows that the dynamical exponents  $\alpha$ ,  $\nu_t$ , and  $z$  do satisfy scaling relations separately for each  $k$ .

## II. MODEL

The model is defined on a one-dimensional periodic lattice of size  $L$  with sites labeled by  $i = 1, 2, \dots, L$ . Each site can be occupied by at most one particle and correspondingly there is a site variable  $s_i = 1, 0$  that represents the presence or absence of the particle at site  $i$ . The dynamics of the model are given by

$$10^k 10^m 1 \rightarrow \begin{cases} 10^{k+1} 10^{m-1} 1 & \text{for } k < n, m \geq 1 \\ 10^{k-1} 10^{m+1} 1 & \text{for } m < n, k \geq 1, \end{cases} \quad (1)$$

\*arijit.chatterjee@saha.ac.in

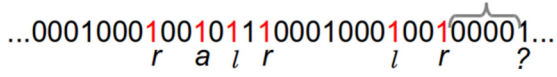


FIG. 1. Schematic description of the model. Particles surrounded from both sides by other particles, or by 0-clusters of size greater than or equal to  $n$ , are inactive, whereas all other particles are active. For  $n = 3$ , the active particles of a typical configuration are marked as  $l$ ,  $r$ , and  $a$  depending on whether they can move to left, right, or in both directions. A 0-cluster of size greater than  $n$  (marked with a bracket) can appear in the initial condition of an active phase, but they eventually disappear as the system reaches the stationary state.

where a particle moves to a vacant nearest neighbor chosen randomly if the move does not increase interparticle separation beyond  $n + 1$  ( $n$  being a fixed integer parameter of the model). Clearly, the total number of particles  $N = \sum_{i=1}^L s_i$ , or equivalently the density  $\rho = N/L$ , is conserved. A schematic description of the dynamics is given in Fig. 1.

Alternatively, the dynamics of the model can be considered as constrained diffusion of hard-core particles. The constraint comes from the fact that the diffusing particle's distance, measured from the nearest particle, does not exceed  $n + 1$ . We further refer to this model as the constrained diffusion model (CDM). In fact, recently, a similar assisted hopping model was introduced and solved exactly [16], where particle hopping depends on the interparticle separation, but unlike CDM particles there can hop by one or *more* steps across the empty regions.

In this constrained diffusion model, a particle that is surrounded from both sides by other particles, or by 0-clusters of size greater than or equal to  $n$ , are inactive as they cannot move; all other particles are active. Thus, the system has many absorbing configurations where all particles are inactive. It is important to note that the dynamics allow a decrement of length of all 0-clusters but an increment of only those having length less than  $n$ . Thus it is evident that when  $\rho \simeq 0$ , i.e., when the average separation between neighboring particles is large, all the small 0-clusters (size less than  $n$ ) of the system tend to grow in size until they reach a maximum  $n$ . In this case, the number of particles is not enough to reorganize the distances between the neighboring particles below  $n + 1$ , forcing the system to fall into an absorbing configuration. On the other hand, for high density the system has a large number of clusters of size less than  $n$  that would grow at the expense of the larger ones, but all of them cannot reach the maximum value  $n$ . Thus, all large clusters (size greater than  $n$ ), if present in the initial state, would eventually be destroyed and the system remains active forever; this is surely the case when  $\rho > \frac{1}{n+1}$ . Clearly, one expects an absorbing phase transition to occur at some density  $\rho \leq \frac{1}{n+1}$ . We see later [in Eq. (14)] that the critical density is in fact  $\rho_c = \frac{1}{n+1}$ .

Let us consider the system with  $\rho > \frac{1}{n+1}$  where the steady state is certainly active. The initial configurations of the system in this case may consist of several 0-clusters of size greater than  $n$ , but all these configurations are *nonrecurring* as the system leaves these configurations by destroying the large clusters and never visits them again. The stationary state of the system only consists of configurations that are *recurring*, where all 0-clusters are of size  $n$  or less. Thereby in the steady state, if

the dynamics (1) allow a particle to move from left to right they also allow the reverse, i.e., a move from right to left. Since both hopping rates are unity, the steady state satisfies the detailed balance condition with a stationary weight  $w(C) = 1$  for all recurring configurations. Thus, representing the configurations as  $C \equiv \{10^{m_1} 10^{m_2} \dots 10^{m_N}\}$ , we have

$$w(\{10^{m_1} 10^{m_2} \dots 10^{m_N}\}) = \begin{cases} 1 & \forall m_i \leq n \\ 0 & \text{otherwise,} \end{cases} \quad (2)$$

where the second step ensures that the steady-state weight of the nonrecurring configurations is zero. The corresponding probability is then

$$P_N(\{s_i\}) = \frac{w(\{s_i\})}{\Omega_N}, \quad \Omega_N = \sum_{\{s_i\}} w(\{s_i\}) \delta\left(\sum_i s_i - N\right). \quad (3)$$

Here  $\Omega_N$  is the number of recurring configurations of a system of size  $L$  having  $N$  particles. It is customary to work in the grand canonical ensemble (GCE) where the density of the system can be tuned by a fugacity  $z$ ; the partition function in the GCE is  $Z = \sum_{N=0}^{\infty} \Omega_N z^N$ . To proceed further, we make an ansatz that the steady-state weights of the configurations can be expressed in the matrix product form

$$w(\{10^{m_1} 10^{m_2} \dots 10^{m_N}\}) = \text{Tr}[DE^{m_1} \dots DE^{m_N}], \quad (4)$$

where matrices  $D$  and  $E$  represent 1 and 0, respectively. All that we need for a matrix formulation to work is to find a representation of  $D$  and  $E$  that correctly generates the steady-state weights given by Eq. (2). The matrix formulation is very useful here, as one can simply set

$$E^m = 0 \quad \text{for } m > n \quad (5)$$

to ensure that the probability of all nonrecurring configurations is 0. Further, let us assume that the matrix  $D = |\alpha\rangle\langle\beta|$ , where  $|\beta\rangle$  and  $\langle\alpha|$  are yet to be determined. Now the recurring configurations are equally likely if

$$\langle\beta|E^m|\alpha\rangle = 1 \quad \text{for } 0 \leq m \leq n. \quad (6)$$

Together, Eqs. (5) and (6) are satisfied by the  $(n + 1)$ -dimensional matrices

$$E = \sum_{k=1}^n |k\rangle\langle k+1|, \quad |\alpha\rangle = \sum_{k=1}^{n+1} |k\rangle, \quad |\beta\rangle = |1\rangle, \\ D = |\alpha\rangle\langle\beta|. \quad (7)$$

Now we can write a grand canonical partition function

$$Z_L(z) = \text{Tr}[T(z)^L] \quad \text{for } T(z) = zD + E, \quad (8)$$

where the fugacity  $z$  controls the particle density  $\rho$ . The weight of the configuration having no particles is  $\text{Tr}[E^L] = 0$  for  $L > n$  [from Eq. (6)]. Thus,  $Z_L(z)$  is the sum of the weights of all other configurations that have at least one particle,

$$Z_L(z) = z \sum_{k=1}^L \text{Tr}[E^{k-1} D T^{L-k}] = z \sum_{k=1}^L \langle\beta|T^{L-k} E^{k-1}|\alpha\rangle. \quad (9)$$

For any specific  $n$ ,  $Z_L(z)$  can be calculated explicitly. We prefer to use a generating function [or partition function] of the

system in the variable length ensemble (VLE)]

$$\begin{aligned}\mathcal{Z}(z, \gamma) &= \sum_{L=1}^{\infty} \gamma^L Z_L(z) = \langle \beta | \frac{\gamma z}{\mathcal{I} - \gamma T} \frac{1}{\mathcal{I} - \gamma E} | \alpha \rangle \\ &= \gamma z \frac{g'(\gamma)}{1 - zg(\gamma)}, \\ g(x) &= \sum_{k=0}^n x^{k+1} = x \frac{x^{n+1} - 1}{x - 1},\end{aligned}\quad (10)$$

which, together with  $z$  and  $\gamma$ , determines the macroscopic variables

$$\begin{aligned}\langle L \rangle &= \frac{\gamma}{\mathcal{Z}} \frac{\partial \mathcal{Z}}{\partial \gamma} = 1 + \gamma z \frac{g'(\gamma)}{1 - zg(\gamma)} + \gamma \frac{g''(\gamma)}{g'(\gamma)}, \\ \langle N \rangle &= \frac{z}{\mathcal{Z}} \frac{\partial \mathcal{Z}}{\partial z} = \frac{1}{1 - zg(\gamma)}.\end{aligned}\quad (11)$$

The thermodynamic limit  $\langle L \rangle \rightarrow \infty$ , where the VLE is expected to be equivalent to the GCE, corresponds to  $z \rightarrow 1/g(\gamma)$ . Also in this limit the particle density is

$$\rho(\gamma) = \frac{\langle N \rangle}{\langle L \rangle} = \frac{1}{\gamma} \frac{g(\gamma)}{g'(\gamma)}.\quad (12)$$

Since both  $g(\gamma)$  and  $\gamma g'(\gamma)$  are polynomials of order  $n+1$  the density  $\rho$  must be finite as  $\gamma \rightarrow \infty$ , which corresponds to the limit  $z \rightarrow 0$ , as  $z = 1/g(\gamma)$ ,

$$\begin{aligned}\lim_{z \rightarrow 0} \rho(z) &\equiv \lim_{\gamma \rightarrow \infty} \rho(\gamma) \\ &= \frac{1}{n+1} + \frac{1}{(n+1)^2} \frac{1}{\gamma} + O\left(\frac{1}{\gamma^2}\right).\end{aligned}\quad (13)$$

This proves that the critical density is

$$\rho_c = \frac{1}{n+1}\quad (14)$$

and the system goes to an absorbing state when  $\rho < \rho_c$ . Further, Eq. (13) indicates that, near the absorbing transition,

$$\gamma^{-1} \simeq (n+1)^2 (\rho - \rho_c).\quad (15)$$

In Fig. 2(a) we have plotted  $\rho$  as a function of  $\gamma^{-1}$  for  $n=2$ , with the inset showing  $z \equiv g(\gamma)^{-1}$  as a function of  $\gamma^{-1}$ . Figure 2(b) shows the plot of  $\rho(z)$ . Clearly, both in the limit  $z \rightarrow 0$  or equivalently when  $\gamma \rightarrow \infty$ ,  $\rho \rightarrow \frac{1}{3}$ , indicating that an absorbing phase transition occurs at  $\rho_c = \frac{1}{3}$ .

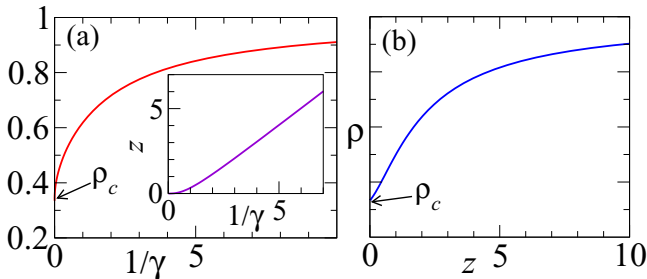


FIG. 2. (a) For  $n=2$ , the density  $\rho$  and the fugacity  $z = g(\gamma)^{-1}$  (inset) are shown as a function of  $\gamma^{-1}$  following Eq. (27). (b) Parametric plot of  $\rho$  as a function of  $z$ .

### III. MULTICRITICALITY

At the critical density  $\rho_c$  all 0-clusters are of length  $n$ . Thus, as  $\rho \rightarrow \rho_c$  from above, i.e., in the active phase  $\rho > \rho_c$ , the number of 0-clusters having size  $k < n$  must individually vanish. Defining the density of such clusters as  $\phi_k$ , we have

$$\begin{aligned}\phi_k &= \langle 10^k 1 \rangle = \frac{\gamma^{k+2} z^2}{\mathcal{Z}(z, \gamma)} \text{Tr} \left[ D E^k D \frac{1}{\mathcal{I} - \gamma T} \right] \\ &= \frac{\gamma^{k+2} z^2}{\mathcal{Z}(z, \gamma)} \langle \beta | E^k | \alpha \rangle \langle \beta | \frac{1}{\mathcal{I} - \gamma T} | \alpha \rangle = \rho z \gamma^{k+1}\end{aligned}\quad (16)$$

for  $0 \leq k < n$ . Here, in the last step we have used the fact that

$$\langle \beta | \frac{1}{\mathcal{I} - \gamma T} | \alpha \rangle = \frac{g(\gamma)}{\gamma - \gamma z g(\gamma)}, \quad \langle \beta | E^k | \alpha \rangle = 1.\quad (17)$$

In the thermodynamic limit  $z \rightarrow g(\gamma)^{-1}$ , we have

$$\phi_k = \rho \frac{\gamma^{k+1}}{g(\gamma)} = \frac{\gamma^k}{g'(\gamma)}\quad (18)$$

and in the critical limit  $\gamma \rightarrow \infty$  [where  $g(\gamma) \simeq \gamma^{n+1}$ ],

$$\phi_k \simeq \gamma^{k-n} \simeq (n+1)^{3-2k} (\rho - \rho_c)^{\beta_k}, \quad \beta_k = n - k.\quad (19)$$

In Fig. 3(a) we have plotted  $\phi_k$  for  $n=2$  as a function of density  $\rho$ . Both  $\phi_0$  and  $\phi_1$  vanish as  $\rho \rightarrow \rho_c = \frac{1}{3}$  and thus each of them can be considered as an order parameter that describes the APT. However,  $\phi_2$  does not vanish and at the critical point  $\phi_2 = (1 - \rho_c)/2$  because there is an exact correspondence  $1 - \rho = \sum_{k=0}^n k \phi_k$  that holds for any  $n$  and  $\gamma$ . Also at  $\gamma = 1$ , which corresponds to the density  $\frac{2}{n+2}$  [from Eq. (12)], all  $\phi_k$  take the same value  $\frac{2}{(n+1)(n+2)}$  [from Eq. (16)]. Thus, for  $n=2$ , the  $\phi_k$  cross each other at  $\rho = \frac{1}{2}$ . In Fig. 3(b) we show  $\phi_k$  as a function of  $\rho - \frac{1}{3}$  in logarithmic scale; both  $\phi_0$  and  $\phi_1$  show power laws as a function of  $\Delta = \rho - \rho_c$  in logarithmic scale, suggesting that  $\phi_{0,1} \sim \Delta^{\beta_{0,1}}$  with  $\beta_0 = 2$  and  $\beta_1 = 1$ .

Returning to the general  $n$ , all the  $\phi_k$  with  $k = 0, 1, \dots, n-1$  vanish as  $\rho \rightarrow \rho_c$  following  $\phi_k \simeq (\rho - \rho_c)^{\beta_k}$  with exponents  $\beta_k = n - k$ . The natural question is then whether other exponents associated with the  $\phi_k$  will be modified such that the standard scaling relations are obeyed. The answer is affirmative, which we will discuss in detail. However, let us recall that, besides these  $n$  observables  $\phi_k$ , there is a natural order parameter  $\rho_a$ , the density of active particles, that

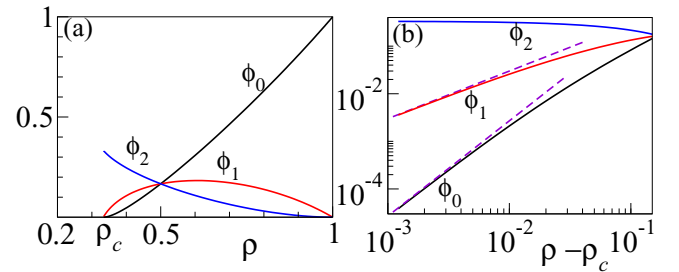


FIG. 3. (a) For  $n=2$ ,  $\phi_k = \langle 10^k 1 \rangle$  are shown as functions of  $\rho$  for  $k=0,1,2$ . Clearly,  $\phi_{0,1}$  vanishes as  $\rho \rightarrow \rho_c = 1/3$ , whereas  $\phi_2 \rightarrow (1 - \rho_c)/2$ . (b) Logarithmic-scale plot of  $\phi_{0,1,2}$  as a function of  $\rho - \rho_c$  with slope  $\beta_k = 2 - k$ . The dashed line corresponds to the near critical approximation of  $\phi_k$ , given by Eq. (19).

conventionally characterizes the APT. Since in the steady state inactive particles are surrounded from both sides by 0-clusters of size 0 or  $n$ , the density of active particles is

$$\rho_a = \sum_{k_1, k_2=0}^n \psi_{k_1, k_2} - \psi_{0,0} - \psi_{n,n}$$

$$\text{for } \psi_{k_1, k_2} = \langle 10^{k_1} 10^{k_2} 1 \rangle = \rho z^2 \gamma^{k_1+k_2+2}, \quad (20)$$

where  $0 \leq k_1$  and  $k_2 \leq n$ . Now, for a thermodynamic system  $z \rightarrow 1/g(\gamma)$  and in the critical limit (as  $\gamma \rightarrow \infty$ ),

$$\rho_a = \frac{\rho}{g(\gamma)^2} [g(\gamma)^2 - \gamma^2 - \gamma^{2n+2}]$$

$$\sim \rho_c(\rho - \rho_c) + O((\rho - \rho_c)^2).$$

Thus, the natural order-parameter exponent associated with  $\rho_a$  is  $\beta = 1$ .

To calculate other static exponents  $\nu$  and  $\eta$  we study the correlation functions, first the density correlation function

$$C(r) = \langle s_i s_{i+r+1} \rangle - \rho^2$$

$$= \frac{\gamma^2 z^2}{\mathcal{Z}(z, \gamma)} \langle \beta | (\gamma T)^r | \alpha \rangle \langle \beta | \frac{1}{\mathcal{I} - \gamma T} | \alpha \rangle - \rho^2$$

$$= \frac{\rho \gamma}{g(\gamma)} \langle \beta | (\gamma T)^r | \alpha \rangle - \rho^2. \quad (21)$$

Similarly, the correlation of the order parameters can be calculated using a variables  $s_i^k$  that takes a nonzero value 1 only when the  $i$ th site is occupied and exactly  $k$  neighbors to its right are vacant (thus  $\phi_k = \langle 10^k 1 \rangle = \langle s^k \rangle$ ),

$$C_k(r) = \langle s_i^k s_{i+r+1}^k \rangle - \phi_k^2 = \frac{\gamma^{2k+4} z^4}{\mathcal{Z}(z, \gamma)} \langle \beta | E^k | \alpha \rangle^2$$

$$\times \langle \beta | (\gamma T)^r | \alpha \rangle \langle \beta | \frac{1}{\mathcal{I} - \gamma T} | \alpha \rangle - \phi_k^2$$

$$= \frac{\rho \gamma^{2k+3}}{g^3(\gamma)} \langle \beta | (\gamma T)^r | \alpha \rangle - \phi_k^2. \quad (22)$$

Clearly, the  $r$  dependence of  $C(r)$  and  $C_k(r)$  comes from the same factor  $\langle \beta | (\gamma T)^r | \alpha \rangle$  and the detailed structure of these correlation functions would depend on the nature of the eigenvalues of  $T$ .

Eigenvalues can be calculated explicitly for any given  $n$ , but first let us extract some general results. The characteristic equation for the eigenvalue equation for  $T$  is

$$\lambda^{n+1} - z \sum_{k=0}^n \lambda^k = 0, \quad (23)$$

which is equivalent to  $z g(\lambda) = \lambda^{n+2}$ . Since  $g(x)$  satisfies an identity  $g(\frac{1}{x}) = \frac{g(x)}{x^{n+2}}$ , using  $z = g(\gamma)^{-1}$  one can check that  $\lambda = \gamma^{-1}$  is one of the solution of the characteristic equation. Again, since the characteristic equation changes sign once, from Descartes' sign rule we conclude that there is exactly one positive real eigenvalue; thus the largest eigenvalue of  $T$  is  $\lambda_1 = 1/\gamma$ . Assuming that the eigenvalues  $\{\lambda_k\}$  are ordered such that  $\lambda_1 < |\lambda_2| \leq \dots \leq |\lambda_{n+1}|$  (the modulus is taken as generically

the eigenvalues could be complex), we write

$$\langle \beta | T^r | \alpha \rangle = A_1 \left( \lambda_1^r + \sum_{k=2}^{n+1} A_k \lambda_k^r \right),$$

where  $A_k$  are constants, independent of  $r$ . Since, the correlation function  $C(r)$  vanishes in the limit  $r \rightarrow \infty$ , we must have  $A_1 = \rho g(\gamma)/\gamma$ , which results in the asymptotic form of the correlation function as

$$C(r) \simeq \rho^2 A_2 (\gamma \lambda_2)^r, \quad C_k(r) \simeq \phi_k^2 A_2 (\gamma \lambda_2)^r. \quad (24)$$

If  $\lambda_2$  is complex, then  $\lambda_3$  must be  $\lambda_2^*$ , because complex roots of real-value polynomials appear pairwise. Taking  $\lambda_{2,3} = \bar{\lambda} e^{\pm i\theta}$ , the correlation functions can be written as

$$C(r) \simeq \rho^2 A_2 (\gamma \bar{\lambda})^r \cos(r\theta),$$

$$C_k(r) \simeq \phi_k^2 A_2 (\gamma \bar{\lambda})^r \cos(r\theta). \quad (25)$$

Let us calculate the correlation functions explicitly for  $n = 2$ , where the eigenvalues of the transfer matrix  $T = zD + E$ , with  $z^{-1} = g(\gamma) = \gamma + \gamma^2 + \gamma^3$  and  $D$  and  $E$  given by Eq. (7) are

$$\lambda = \left\{ \frac{1}{\gamma}, \bar{\lambda} e^{\pm i\theta} \right\}, \quad \bar{\lambda} = \frac{\gamma}{g(\gamma)},$$

$$\tan(\theta) = \frac{\sqrt{3 + 2\gamma + 3\gamma^2}}{1 + \gamma}. \quad (26)$$

This leads to

$$\rho = \frac{1 + \gamma + \gamma^2}{1 + 2\gamma + 3\gamma^2}, \quad \phi_k = \frac{\gamma^k}{1 + 2\gamma + 3\gamma^2}. \quad (27)$$

Thus, in this case the spatial correlation functions would show damped oscillations of period  $2\pi/\theta$ . We calculate the density correlation functions of the CDM with  $n = 2$  at density  $\rho = \frac{10}{29} \simeq 0.345$ , which is close to the critical density  $\rho_c = 1/3$ , and plot  $C(r)$  as a function of  $r$  in Fig. 4. We compare this with the analytic results, using  $\gamma = 10.8$  [corresponding to  $\rho = \frac{10}{29}$  in Eq. (25)]. The oscillations are consistent with  $\theta = 1.03$  calculated from Eq. (26).

It is important to note that, for any  $n$ , all  $C_k(r)$ s have the same  $r$  dependence, suggesting a unique length scale

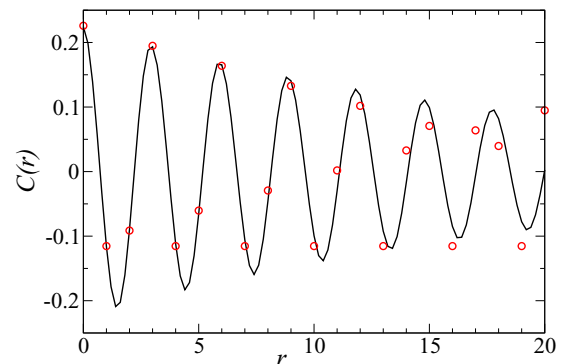


FIG. 4. For  $n = 2$ , the density correlation function  $C(r)$  calculated from Monte Carlo simulations for  $\rho = \frac{10}{29} \simeq 0.345$ , a value closer to the critical density  $\rho_c = 1/3$ , is compared with the analytical results calculated using Eqs. (25)–(27).

$\xi = 1/\ln(\gamma\bar{\lambda})$ . At the critical point  $\gamma \rightarrow \infty$ , the eigenvalues  $\lambda_k$  approach  $\frac{1}{\gamma}e^{2\pi ik/(n+1)}$  and thus  $|\lambda_k|/\lambda_1 \rightarrow 1$ , resulting in a diverging correlation length  $\xi$ . Near the critical point, we may write, to leading order,  $\gamma\bar{\lambda} - 1 \propto \frac{1}{\gamma}$ ; thus, the correlation length  $\xi \sim \gamma \sim (\rho - \rho_c)^{-\nu}$ , with  $\nu = 1$ . Also, since the correlation functions are expected to decay as  $r^{-(d-2+\eta)}$ , for this one-dimensional model ( $d = 1$ ) we get  $\eta = 1$ .

Now let us turn our attention to the dynamic exponents at the critical point. At the critical point, every particle has exactly  $n$  vacant sites to their right. If we add an extra particle, it will break one of the 0-clusters into two, each having size less than  $n$ , creating some active particles in the system. It is easy to see that these active particles would perform an unbiased random walk, exploring a typical region of size  $\sqrt{t}$  in time  $t$ . Thus, the dynamic exponent is  $z = 2$ . Now assuming that the scaling relations  $\nu_t = \nu z$ , we expect  $\nu_t = 2$ .

Since the  $\phi_k$  vanish at the critical point, it is natural to expect that their decay from an active initial condition follows a power law

$$\phi_k(t) \sim t^{-\alpha_k}, \quad \alpha_k = \frac{\beta}{\nu_t} = \frac{n-k}{2}. \quad (28)$$

Of course, we have assumed scaling relations to hold here, while their validity is doubted [17,23,25] in similar models. Thus it is necessary that we verify from numerical simulations whether the scaling relations are indeed valid here.

To measure the decay exponents at the critical density  $\rho_c$  corresponding to any  $\phi_k$ , one must carefully choose initial configurations with some nonzero  $\phi_k$  that possesses natural correlations of the critical state. It has been argued [22,24] and verified in many models of the APT [23,26] that the critical absorbing state is hyperuniform, i.e., the variance of density in the critical state is sublinear in volume (here length  $L$ ). Usually densities in hyperuniform states are anticorrelated and thus it is useful to study decay from configurations that already possess the natural correlations of the critical state. Such natural initial conditions can be generated following the prescriptions given in Ref. [22]. In the restricted diffusion model, starting from the absorbing configuration, 1s separated by 0s, we allow particles to diffuse stochastically for a very short time (say, 0.1 Monte Carlo step) to create an active state and then turn on the dynamics. The decay of  $\phi_k(t)$  for  $n = 2$  and 3 is plotted in Figs. 5(a) and 5(b), respectively, in logarithmic scale; they show that  $\alpha_k = (n-k)/2$  consistently.

We also calculate the dynamical exponent  $z$  from the finite-size corrections. At the transition point,

$$\phi_k(t, L) = t^{-\alpha} \mathcal{F}_k\left(\frac{t}{L^z}\right). \quad (29)$$

Starting from the natural initial condition, we measure  $\phi_k(t, L)$  for different  $L$  and plot  $\phi_k(t, L)t^{\alpha_k}$  as a function of  $\frac{t}{L^z}$  in Figs. 6(a) and 6(b), respectively, for  $k = 0$  and 1, taking  $z = 2$ . A good data collapse confirms that  $z = 2$ . Note that the fluctuations and a small deviation of  $\alpha_0 = 1.02$  from the expected value 1 can be blamed on the small numerical value of  $\phi_0$ .

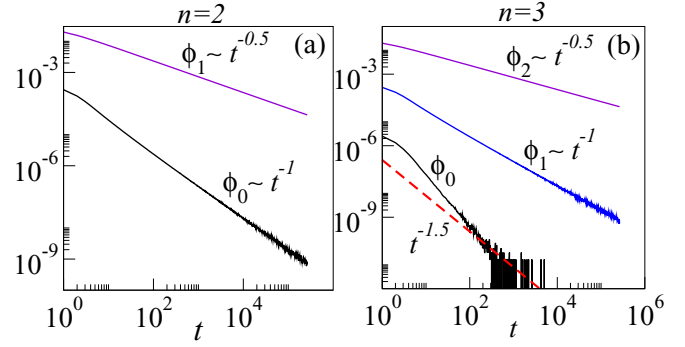


FIG. 5. At the critical point the order parameters  $\phi_k(t)$  for  $k = 0, 1, \dots, n-1$  decay as  $t^{-\alpha_k}$ , where  $\alpha_k = \frac{n-k}{2}$ . The decay of  $\phi_k(t)$ , from a natural initial condition (see the text for details), is shown for (a)  $n = 2$  and (b)  $n = 3$  for system size  $3 \times 2^{14}$  and  $2^{16}$ , respectively.

#### IV. MAPPING TO THE MISANTHROPE PROCESS

We must mention that the CDM can be mapped to the misanthrope process in one dimension [27], where particles do not obey the hard-core restriction and hop, one at a time, from a site (usually called a box) to one of the neighbors with a rate that depends on the occupation number of both the departure and the arrival site. In this mapping, 1s are considered as boxes carrying exactly as many particles as the number of vacant sites in front them. Thus, the dynamics of the CDM translates to hopping of a single particle from a box to a neighbor with a restriction that the hopping must not increase the occupation of the target box beyond  $n$ . Thus the system falls into an absorbing state (where all boxes contain  $n$  or more particles) when particle per box  $\eta = (L - N)/N$  exceeds  $\eta_c = n$ . Thus, in the active phase all boxes contain less than or equal to  $n$  particles and the partition function in the GCE is  $Z(x) = F(x)^L$ , where  $F(x) = \sum_{k=0}^n x^k$ . The corresponding density is then  $\eta(x) = \frac{1}{F(x)} \sum_{k=0}^n kx^k$ . The order parameters  $\phi_k$  are simply the steady-state probability that a box contains  $k$  particles;  $\phi_k = x^k/F(x)$  vanish as  $x^{k-n}$  in the limit  $x \rightarrow \infty$ , or equivalently  $\phi_k \sim (n - \eta)^{n-k}$  as in this limit  $\eta \sim n - 1/x$ . Although the  $\phi_k$  can be calculated efficiently in the box

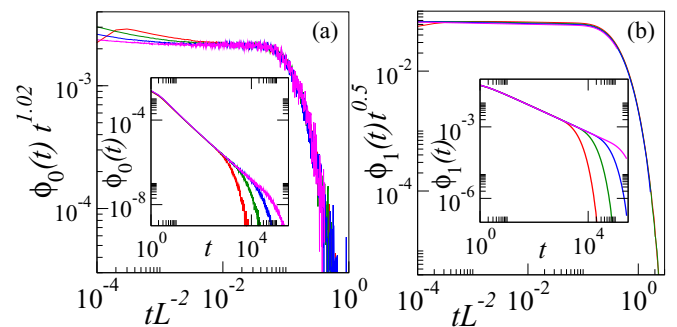


FIG. 6. Scaling collapse of order parameters  $\phi_{0,1}$  for  $n = 2$  following Eq. (29). At the critical point,  $\phi_k(t)t^{\alpha_k}$  is a universal function of  $tL^{-z}$ . Data collapse is shown for (a)  $k = 0$  and (b)  $k = 1$  for system size  $L = 300 \times (1, 2, 4, 8)$ . Here we take  $z = 2$  and use  $\alpha_k$  as a fitting parameter. data collapse is observed for (a)  $\alpha_0 = 1.02$  and (b)  $\alpha_1 = 0.5$ .

particle picture, it is rather difficult to calculate the correlation functions in general, as the information about particle ordering is lost in the mapping. In such cases, it is useful to write the steady state in matrix product form [28], whenever possible.

## V. SUMMARY

We have studied diffusion of hard-core particles on a one-dimensional periodic lattice, where particle movement is constrained such that the interparticle separation is not increased beyond  $n + 1$ . Thus particles that are surrounded from both sides either by other particles or by 0-clusters of size greater than or equal to  $n$  are immobile or inactive, whereas all other particles are active. Thus the initial distances between two neighboring particles, if larger than  $n + 1$ , can only decrease if one of the particle is active. This constrained diffusion model undergoes an absorbing state phase transition when the density is lowered below a critical value  $\rho_c = \frac{1}{n+1}$ . Interestingly, besides the activity density  $\rho_a$ , the APT here can be characterized by the steady-state densities of 0-clusters of size  $0 \leq k < n$  (i.e.,  $\phi_k = \langle 10^k 1 \rangle = \langle s_i^k \rangle$ ) that vanish simultaneously at  $\rho_c$ . We show that the steady state of the CDM can be written as a matrix product, which helps us obtain the static critical exponents exactly:  $\rho$  approaches  $\rho_c$  from the active side,  $\rho_a \sim (\rho - \rho_c)^\beta$  with  $\beta = 1$ , and other order parameters vanish as  $\phi_k \sim (\rho - \rho_c)^{\beta_k}$  with  $\beta_k = n - k$ . This multicritical behavior is characterized by correlation exponents  $\nu = 1 = \eta$ , which are the same for all  $\phi_k$  as  $\langle s_i^k s_{i+r}^k \rangle \sim e^{-r/\xi}$  with  $\xi \sim (\rho - \rho_c)^{-1}$ . The steady-state dynamics of the CDM in the active phase is only unbiased diffusion of particles, leading to

an dynamical exponent  $z = 2$ . Thus, assuming that the scaling relations  $\nu_l = z\nu$  and  $\alpha = \beta/\nu_l$  hold, one expects that  $\nu_l = 2$  is independent of  $k$  whereas  $\alpha \equiv \alpha_k = (n - k)/2$ . We verified the scaling relations explicitly from careful Monte Carlo simulations of the model by measuring  $z$  and  $\alpha_k$  for  $n = 2, 3$ . In these simulations, the major difficulty is to choose initial conditions that retain natural correlations of the stationary state, which we overcome by using natural initial conditions [22].

Multicritical phase transitions are not specific to absorbing phase transitions. It has been observed in many other contexts, like in eight-vertex and solid-on-solid models [29,30], the  $N$ -state chiral Potts model [31], antiferromagnetic spin chains [32], etc. Also, this has been observed in the multispecies directed percolation process [11] and in growth models with adsorption [13]. In all these models, the critical point could be characterized by many order parameters, each corresponding to a particular kind of order, but they all vanish at the same critical point. Exactly solvable models are a step forward in understanding the nature of the transition. It would be interesting to look for perturbations that could produce different ordered phases of the CDM at different densities.

## ACKNOWLEDGMENTS

The authors acknowledge Amit K. Chatterjee for helpful discussions. P.K.M. thankfully acknowledge financial support from the Science and Engineering Research Board, India (Grant No. EMR/2014/000719).

- 
- [1] M. Henkel, H. Hinrichsen, and S. Lübeck, *Non-Equilibrium Phase Transitions* (Springer, Berlin, 2008), Vol. 1.
- [2] H. Hinrichsen, *Adv. Phys.* **49**, 815 (2000).
- [3] P. Grassberger, *Phys. Rev. E* **59**, R2520 (1999).
- [4] P. Grassberger, *J. Stat. Phys.* **79**, 13 (1995).
- [5] F. D. A. A. Reis, *Braz. J. Phys.* **33**, 501 (2003).
- [6] F. Z. Schlögl, *Physica A* **53**, 147 (1972); R. M. Ziff, E. Gulari, and Y. Barshad, *Phys. Rev. Lett.* **56**, 2553 (1986); D. A. Brown and P. Kleban, *Appl. Phys. A* **51**, 194 (1990).
- [7] E. V. Albano, *J. Phys. A* **27**, L881 (1994).
- [8] A. Lipowski and M. Lopata, *Phys. Rev. E* **60**, 1516 (1999).
- [9] K. A. Takeuchi, M. Kuroda, H. Chaté, and M. Sano, *Phys. Rev. Lett.* **99**, 234503 (2007); *Phys. Rev. E* **80**, 051116 (2009).
- [10] H. K. Jenssen, *Z. Phys. B* **42**, 151 (1981); P. Grassberger, *ibid.* **47**, 365 (1982).
- [11] U. C. Täuber, M. J. Howard, and H. Hinrichsen, *Phys. Rev. Lett.* **80**, 2165 (1998).
- [12] R. Chatterjee, P. K. Mohanty, and A. Basu, *J. Stat. Mech.* (2011) L05001; S.-C. Park, *ibid.* (2011) L09001.
- [13] U. Alon, M. R. Evans, H. Hinrichsen, and D. Mukamel, *Phys. Rev. Lett.* **76**, 2746 (1996).
- [14] J. A. Plascak, *Physica A* **198**, 655 (1993); O. D. R. Salmon and F. D. Nobre, *Phys. Rev. E* **89**, 062104 (2014).
- [15] B. Nienhuis, S. O. Warnaar, and H. W. J. Blöte, *J. Phys. A* **26**, 477 (1993); J. L. Cardy, M. Nauenberg, and D. J. Scalapino, *Phys. Rev. B* **22**, 2560 (1980).
- [16] R. Dandekar and D. Dhar, *Europhys. Lett.* **104**, 26003 (2013).
- [17] M. Rossi, R. Pastor-Satorras, and A. Vespignani, *Phys. Rev. Lett.* **85**, 1803 (2000).
- [18] A. Vespignani, R. Dickman, M. A. Munoz, and S. Zapperi, *Phys. Rev. E* **62**, 4564 (2000).
- [19] R. Dickman, L. T. Rolla, and V. Sidoravicius, *J. Stat. Phys.* **138**, 126 (2010).
- [20] M. J. de Oliveira, *Phys. Rev. E* **71**, 016112 (2005).
- [21] U. Basu and P. K. Mohanty, *Phys. Rev. E* **79**, 041143 (2009).
- [22] M. Basu, U. Basu, S. Bondyopadhyay, P. K. Mohanty, and H. Hinrichsen, *Phys. Rev. Lett.* **109**, 015702 (2012).
- [23] S. Bondyopadhyay, *Phys. Rev. E* **88**, 062125 (2013); S. Kwon and J. M. Kim, *ibid.* **90**, 046101 (2014).
- [24] D. Hexner and D. Levine, *Phys. Rev. Lett.* **114**, 110602 (2015).
- [25] S. B. Lee and S.-G. Lee, *Phys. Rev. E* **78**, 040103(R) (2008).
- [26] P. Grassberger, D. Dhar, and P. K. Mohanty, *Phys. Rev. E* **94**, 042314 (2016).
- [27] M. R. Evans and B. Waclaw, *J. Phys. A* **47**, 095001 (2014).
- [28] U. Basu and P. K. Mohanty, *J. Stat. Mech.* (2010) L03006.
- [29] G. E. Andrews, R. J. Baxter, and P. J. Forrester, *J. Stat. Phys.* **35**, 193 (1984).
- [30] D. A. Huse, *Phys. Rev. B* **30**, 3908 (1984).
- [31] G. Albertine, B. M. McCoy, J. H. H. Perk, and S. Tang, *Nucl. Phys. B* **314**, 741 (1989); *Int. J. Mod. Phys. A* **14**, 3921 (1999).
- [32] K. Damle and D. A. Huse, *Phys. Rev. Lett.* **89**, 277203 (2002).